

HEMATOPOIESIS AND STEM CELLS

The bulk of the hematopoietic stem cell population is dispensable for murine steady-state and stress hematopoiesis

Kristina B. Schoedel,¹ Mina N. F. Morcos,¹ Thomas Zerjatke,² Ingo Roeder,² Tatyana Grinenko,³ David Voehringer,⁴ Joachim R. Göthert,⁵ Claudia Waskow,⁶ Axel Roers,¹ and Alexander Gerbaulet¹

¹Institute for Immunology, ²Institute for Medical Informatics and Biometry, and ³Department for Clinical Pathobiochemistry, Institute of Clinical Chemistry and Laboratory Medicine, Carl Gustav Carus Faculty of Medicine, Technische Universität Dresden, Dresden, Germany; ⁴Department of Infection Biology, University Hospital Erlangen, Erlangen, Germany; ⁵Department of Hematology, University Hospital of Essen, Essen, Germany; and ⁶Regeneration in Hematopoiesis, Institute for Immunology, Carl Gustav Carus Faculty of Medicine, Technische Universität Dresden, Dresden, Germany

Key Points

- After induced HSPC depletion, HSC numbers remain at low levels whereas progenitors show robust recovery.
- Despite low HSC numbers, hematopoiesis proceeds normally without increased proliferation of the few residual HSCs.

Long-term repopulating (LT) hematopoietic stem cells (HSCs) are the most undifferentiated cells at the top of the hematopoietic hierarchy. The regulation of HSC pool size and its contribution to hematopoiesis are incompletely understood. We depleted hematopoietic stem and progenitor cells (HSPCs) in adult mice *in situ* and found that LT-HSCs recovered from initially very low levels (<1%) to below 10% of normal numbers but not more, whereas progenitor cells substantially recovered shortly after depletion. In spite of the persistent and massive reduction of LT-HSCs, steady-state hematopoiesis was unaffected and residual HSCs remained quiescent. Hematopoietic stress, although reported to recruit quiescent HSCs into cycle, was well tolerated by HSPC-depleted mice and did not induce expansion of the small LT-HSC compartment. Only upon 5-fluorouracil treatment was HSPC-depleted bone marrow compromised in reconstituting hematopoiesis, demonstrating that HSCs and early progenitors are crucial to compensate myeloablation. Hence, a contracted HSC compartment cannot recover *in situ* to its original size, and

normal steady-state blood cell generation is sustained with <10% of normal LT-HSC numbers without increased contribution of the few residual cells. (*Blood*. 2016;128(19):2285-2296)

Introduction

The hematopoietic system continuously produces enormous numbers of mature blood cells. Bone marrow (BM)-resident hematopoietic stem cells (HSCs) are the most undifferentiated cells in the hematopoietic system and give rise to a series of rapidly proliferating precursor populations.^{1,2} The hierarchy of hematopoietic stem and progenitor cell (HSPC) populations was largely established by transplantation of purified BM cell subsets into myeloablated recipients.³ The cells at the top of this hierarchy, defined by their unique capability to long-term repopulate irradiated recipient mice, are designated long-term repopulating (LT)-HSCs² and are endowed with remarkable proliferative potential.

Alongside a quiescent fraction of about 20% to 30% of the HSC population that was found to cycle only every 150 to 200 days, a larger population of “homeostatic” HSCs was supposed to continuously maintain hematopoiesis by cell divisions every 20 to 30 days.^{4,5} HSCs were shown to be awakened from quiescence by cytokines, including interferon α ,⁶ interferon γ ,⁷ and granulocyte colony-stimulating factor⁸ (G-CSF), to meet increased demand in situations of emergency including infection and blood loss. These findings established a concept of continuously active participation of HSCs in steady-state blood cell production and a central role of these cells in emergency hematopoiesis. Two studies,^{9,10} however, recently reported *in vivo* cell-fate tracking in the hematopoietic system and showed that LT-HSC contribution to

hematopoiesis is much less than previously estimated and predicted that steady-state hematopoiesis should continue to function normally in mice in the absence of LT-HSCs.

Here, we directly tested this prediction by induced depletion of LT-HSCs and primitive progenitors *in vivo*. Unexpectedly, LT-HSCs recovered to only a few percent of normal numbers within the first weeks after efficient depletion and then remained at this low level, whereas progenitor populations quickly reexpanded. This persistent reduction of LT-HSC numbers did not compromise steady-state blood cell generation for at least 1 year. The few residual LT-HSCs remained quiescent and their proliferation rate was unchanged. Even hematopoietic stressors known to cause HSC activation were tolerated by HSPC-depleted animals, demonstrating that steady-state and even stress hematopoiesis do not depend on contribution of the LT-HSC compartment.

Methods

Animals

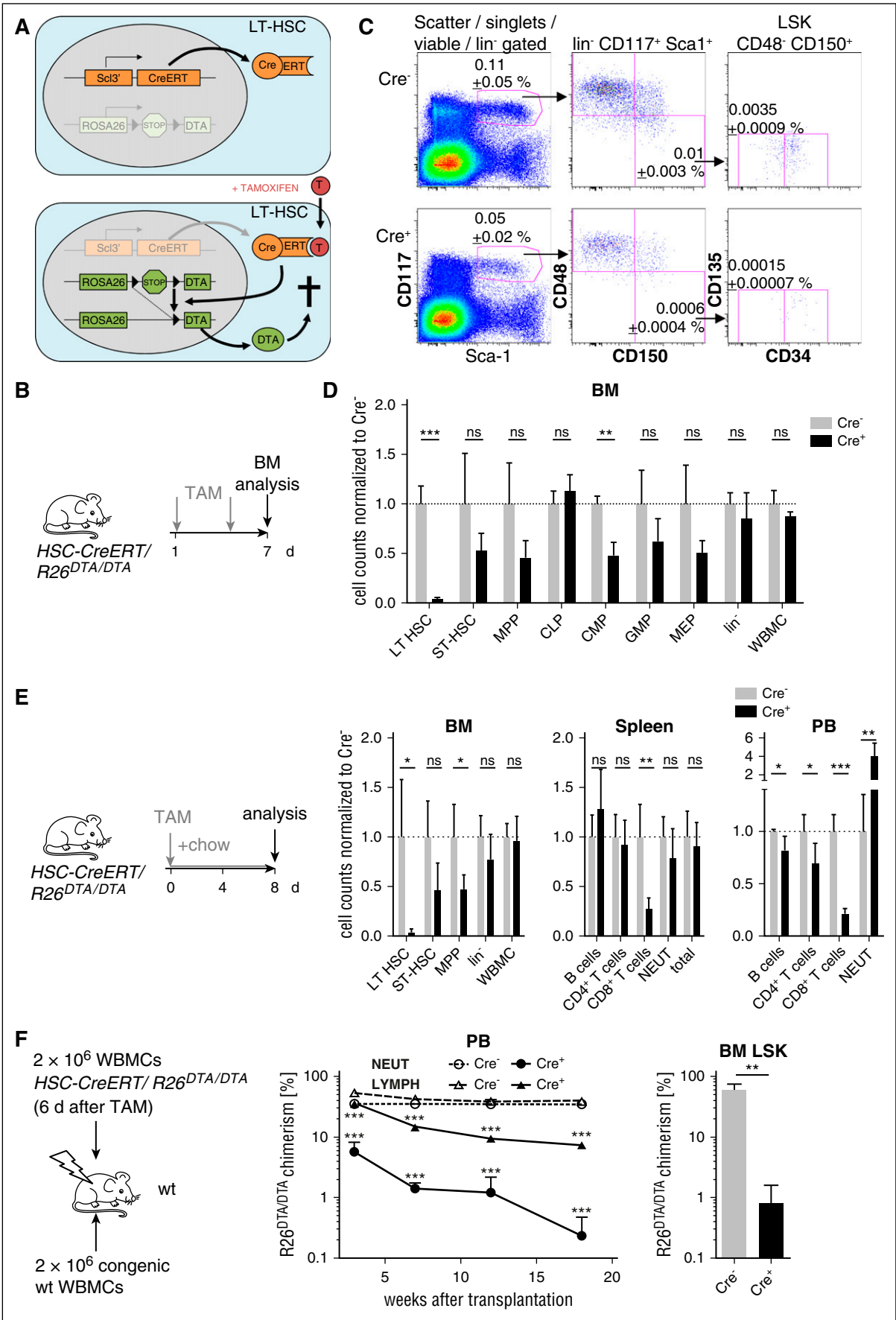
HSC-CreERT/R26^{DTA} mice were generated by crossing *R26^{DTA}* (Gt(ROSA)26Sor^{tm1(DTA)Lky})¹¹ and *HSC-CreERT* (Tg(Tal1-cre/ERT)42-056Jrg) mice.¹²

Submitted 18 March 2016; accepted 22 June 2016. Prepublished online as *Blood* First Edition paper, 29 June 2016; DOI 10.1182/blood-2016-03-706010.

The online version of this article contains a data supplement.

The publication costs of this article were defrayed in part by page charge payment. Therefore, and solely to indicate this fact, this article is hereby marked “advertisement” in accordance with 18 USC section 1734.

© 2016 by The American Society of Hematology



The following mouse strains were additionally used: *R26^{EYFP}* (Gt(ROSA)26Sor^{tm1(EYFP)Cos}),¹³ *R26^{RFP}* (Gt(ROSA)26Sor^{tm1Hij}),¹⁴ B6.CD45.1 (B6.SJL-Ptprc^a Pepc^b/BoyJ),¹⁵ and *R26^{rTA}/Col1a1^{tetO-H2B-RFP}* (Gt(ROSA)26Sor^{tm1(rTA**M2*)Jae}/Col1a1^{tm1(tetO-mCherry)Eggn}).¹⁶ *HSC-CreERT* *R26^{EYFP}* Cre-excision reporter mice were generated by mating *HSC-CreERT* mice to *R26^{EYFP}* animals. Mice with ubiquitous expression of red fluorescent protein (RFP) (B6.ubiRFP) or enhanced yellow fluorescent protein (EYFP) (B6.ubiEYFP) were derived from *R26^{RFP}* or *R26^{EYFP}* animals by breeding to *pgk-Cre* animals (Tg(Pgk1-cre)1Lni).¹⁷ All animals were maintained on C57BL/6 genetic background and kept under specific pathogen-free conditions. All animal experiments were done according to institutional guidelines and were approved by Landesdirektion Dresden (ref. no. 24-9168.11-1/2012-39).

Tamoxifen induction

One to 2 weeks before start of tamoxifen (TAM) administration, mice were kept on a low phytoestrogen standard diet (LASvendi, Solingen, Germany). TAM tablets (30 mg; Ratiopharm, Ulm, Germany) were dissolved overnight in lipid emulsion (SMOFlipid; Fresenius Kabi, Bad Homburg, Germany). TAM solution (20 mg/mL) was applied by oral gavage using a syringe and feeding needle at doses of 0.1 to 0.3 mg/g body weight (BW) to animals at the age of 8 to 12 weeks. In some experiments, mice were additionally fed TAM-containing (400 mg/kg) chow (LASvendi).

Treatments of mice

5-Fluorouracil (5-FU) (150 μ g/g BW; Applichem, Darmstadt, Germany) was administered via intravenous (IV) or intraperitoneal (IP) injection. Two doses of polyinosinic-polycytidylic acid (pI:C) (5 μ g/g BW, first and third day; Invivogen, Toulouse, France) were injected IP. Two doses of phenylhydrazine (PHZ) (40 μ g/g BW, first and second day; Sigma-Aldrich, Schnelldorf, Germany) were injected IP. Five doses of filgrastim (recombinant human G-CSF, 0.3 μ g/g BW daily; Amgen, Munich, Germany) were subcutaneously injected. For platelet depletion, mice were IP injected once with 1.5 μ L/g BW of rabbit anti-mouse thrombocyte serum (Accurate Chemical, Westbury, NY). Histone H2B-RFP expression was induced by providing doxycycline (Dox) (1 mg/mL; Applichem) containing drinking water supplemented with 1% (wt/vol) sucrose for 8 weeks.

BM transplantation

Recipient mice received a single dose of 9 Gy total body irradiation (Yxlon Maxi Shot Source, Hamburg, Germany). Donor cells were administered via IV injection into the retroorbital sinus. Recipient mice received neomycin via drinking water (1.17 g/L) for 3 weeks after γ -irradiation.

In order to determine the frequency of LT repopulating cells, limiting dilutions of whole BM cells (WBMCs) from TAM-induced *HSC-CreERT/R26^{DTA/DTA}* mice were transplanted either directly or 13 weeks after induction alongside with 2×10^5 B6.CD45.1 competitor WBMCs into irradiated B6.CD45.1/CD45.2 recipients. Sixteen to 22 weeks after transplantation, recipient peripheral blood (PB) T lymphocytes (CD3⁺), B lymphocytes (B220⁺), and neutrophils (CD11b⁺, Gr-1^{hi}) were analyzed for their donor origin using a MACSquant flow cytometer (Miltenyi Biotec, Bergisch-Gladbach, Germany). Mice showing $\geq 0.01\%$ *HSC-CreERT/R26^{DTA/DTA}* multilineage chimerism (each T-cell, B-cell, and neutrophil population $\geq 0.01\%$ donor-derived cells) were scored as LT repopulated. Frequency of LT repopulating cells was calculated using ELDA software.¹⁸

Cell preparation

BM cells were isolated by crushing or flushing long bones using phosphate-buffered saline (PBS)/2% fetal calf serum (FCS; Biochrom, Berlin, Germany)/2 mM EDTA and filtered through a 100- μ m mesh. After erythrocyte lysis in NH₄Cl buffer, cells were filtered through a 40- μ m mesh.

PB was drawn into glass capillaries by retrobulbar puncture. For chimerism analysis, blood was flushed out of the capillary using PBS/heparin (250 units/mL; Biochrom). Erythrocyte lysis in NH₄Cl buffer was performed twice for 5 minutes. For hemograms, blood was drawn by retrobulbar puncture directly into EDTA-coated tubes (Sarstedt, Nuembrecht, Germany) and analyzed on a Sysmex XT-2000i Vet analyzer (Sysmex, Norderstedt, Germany).

Spleen cell suspensions were prepared by gently rubbing the entire spleen through a 40- μ m cell strainer. After erythrocyte lysis, cells were filtered through a 40- μ m mesh.

Endosteal cells were isolated as described¹⁹ with minor modifications. Briefly, long bones were collected and crushed in PBS/2% FCS using mortar and pestle. After depletion of BM cells by washing with PBS/2% FCS, bone fragments were incubated with type I collagenase (3 mg/mL; Worthington, Cellsystems, Troisdorf, Germany) in Dulbecco modified Eagle medium with 10% FCS at 37°C, shaking at 1400 rpm in an Eppendorf thermomixer (Hamburg, Germany) for 60 minutes. After digestion, the supernatant was filtered through a 100- μ m mesh, followed by erythrocyte lysis. Cell populations were resolved by flow cytometry (supplemental Figure 1C, available on the Blood Web site).

Flow cytometry

Cells were incubated with antibodies in PBS/2% FCS for 30 minutes, washed twice with PBS/2% FCS, and analyzed on a FACSCalibur, LSR II, ARIA II SORP, or ARIA III (BD Biosciences, Heidelberg, Germany). Data were analyzed using FlowJo V9 software (Tree Star, Ashland, OR) and gates were set according to fluorescence-minus-one controls.

For a detailed overview of antibody clones and gating strategies, refer to supplemental Figures 1 and 4C and supplemental Table 2. Absolute numbers of BM, spleen, and endosteal cells were determined on a MACSquant flow cytometer (Miltenyi Biotec) using propidium iodide staining for dead cell exclusion.

Cell sorting was performed on FACS ARIA III (BD Biosciences). Aliquots of sorted lineage[−]Scal⁺CD117⁺ (LSK) CD48[−]CD150⁺CD34[−]CD135[−] LT-HSCs were reanalyzed (purity >95%).

For analysis of cell cycle, WBMCs were immunomagnetically enriched using anti-CD117 microbeads (Miltenyi Biotec). After extracellular antibody staining, cells were fixed and permeabilized using Cytofix/Cytoperm (BD Biosciences), followed by intracellular staining with anti-Ki-67 and FxCycle Violet dye (Thermo Fisher, Waltham, MA). Cells were analyzed on a FACS ARIA III flow cytometer (BD Biosciences). For gating strategy, see supplemental Figure 1D.

Statistics

See supplemental Methods.

Figure 1. Inducible HSPC depletion. (A) Mouse model for inducible HSPC depletion; a conditional *Rosa26-DTA* knock-in allele (*R26^{DTA}*) was crossed into *HSC-CreERT* mice. In the latter, the TAM-inducible Cre/estrogen receptor fusion protein (CreERT) is expressed in LT-HSCs and to a lower extent in progenitors. Induction of Cre-mediated recombination by TAM triggers expression of DTA in HSPCs and, thereby, their apoptotic cell death. *ScfE5-CreERT-3' enhancer* transgenic mice were designated *HSC-CreERT* throughout the manuscript. (B) *HSC-CreERT/R26^{DTA/DTA}* mice were induced by oral gavage of 2×0.1 mg/g BW TAM. (C) Flow cytometric analysis of BM HSPCs on day 7 after initiation of TAM. One Cre[−] control (Cre[−]) and 1 *HSC-CreERT⁺R26^{DTA/DTA}* (Cre⁺) animal representative of 4 mice per group are shown. Mean frequencies \pm SD of the gated population within WBMCs are shown. (D) Total numbers of HSCs and progenitors recovered from 2 femora and 2 tibiae of the animals described in panel B and shown in panel C. Mean numbers of controls (displayed \pm SD) were set to 1 (dotted line). See supplemental Figure 1A for gating strategies and Figure 1E and supplemental Figure 2A-B for alternative TAM-induction protocols. (E) BM, spleen, and PB of *HSC-CreERT/R26^{DTA/DTA}* were analyzed 8 days after TAM administration ($n = 5$, normalization and display of data as in panel D). (F) WBMCs from TAM-induced (5×0.3 mg/g BW) *HSC-CreERT/R26^{DTA/DTA}* were mixed with equal numbers of B6.CD45.1 competitor WBMCs and transplanted into irradiated B6.CD45.1/CD45.2 recipients ($n = 5$ per genotype). Recipients were monitored for contribution of the *R26^{DTA/DTA}* donor (Cre⁺ or Cre[−]) to PB neutrophils (NEUT, CD11b⁺Gr-1^{hi}) and lymphoid cells (LYMPH, FSC^oSSC^oCD11b⁺Gr-1[−]) as well as to BM LSK cells (18 weeks after transfer). Means \pm SD are shown. Experiment representative of 2 individual replicates. CLP, common lymphocyte progenitor; FSC, forward scatter; GMP, granulocyte/macrophage progenitor; MEP, megakaryocyte/erythrocyte progenitor; ns, not significant; SD, standard deviation; SSC, side scatter.

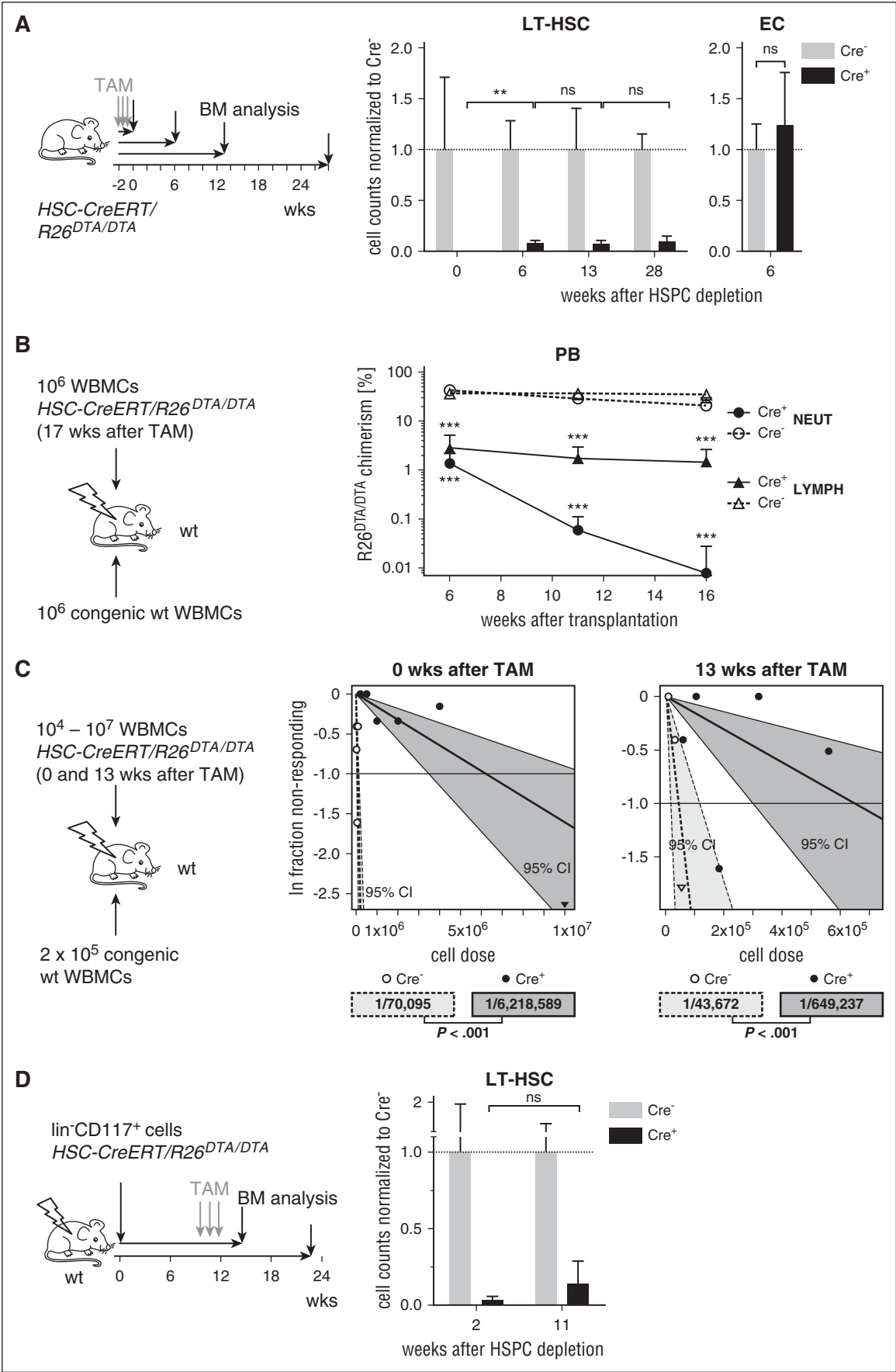


Figure 2.

Results

Inducible depletion of LT-HSCs and progenitors

In order to deplete HSCs and progenitors in vivo, we followed a genetic strategy allowing for controlled suicidal expression of diphtheria toxin A (DTA) with high efficiency in LT-HSCs (Figure 1A). *HSC-CreERT⁺R26^{DTA/DTA}* and *Cre⁻R26^{DTA/DTA}* control mice (see “Methods”) were induced by oral administration of TAM (Figure 1B). Seven days after start of induction, BM was harvested for quantification of HSPCs. Numbers of immunophenotypic LT-HSCs^{4,20} recovered in total from both femora and both tibiae were reduced to 4% of control numbers (Figure 1C-D). Short-term (ST)-HSCs, multipotent progenitors²¹ (MPPs), and common myeloid progenitors²² (CMPs) were reduced by about 50% whereas the lineage-negative (*lin⁻*) population and WBMcs were not significantly altered (see supplemental Figure 1 for gating strategies). In general, the reduction of progenitor cells decreased with more mature immunophenotype. Additional experiments using either the *R26^{DTA}* allele or the *R26^{EYFP}* Cre excision reporter demonstrated that recombination efficiency of HSC and progenitor populations was dependent on TAM dosage and duration of administration as well as zygosity of the *R26* alleles (Figure 1E; supplemental Figure 2A-C), and depletion of immunophenotypic LT-HSCs can approach 100% (Figure 2A; supplemental Figure 2A-B). TAM induction had no significant effects on BM populations in *Cre⁻* and *Cre⁺R26^{wt/wt}* control mice (supplemental Figure 2B). The repopulation activity of CreERT-recombined EYFP⁺ LT-HSCs purified from TAM-induced *HSC-CreERT⁺R26^{EYFP/EYFP}* mice matched unrecombined control LT-HSCs, excluding significant CreERT-related genotoxicity (supplemental Figure 2D). In the absence of TAM, we did not observe HSPC depletion or activation of the *R26^{EYFP}* reporter (supplemental Figure 2E). Analysis of PB, spleen, or peritoneal cell populations (Figure 1E; supplemental Figure 2A,F) did not reveal any reduction of mature hematopoietic cells after TAM induction, except for a complete depletion of mast cells and partial loss of T cells caused by known activity of the promoter *Scl* 3' enhancer in these cell types.^{12,23} By competitively transplanting WBMcs from TAM-induced *HSC-CreERT/R26^{DTA/DTA}* and wild-type (wt) animals into irradiated recipients (Figure 1F), we confirmed severe reduction of functional LT-HSC repopulation activity in HSPC-depleted mice.

We next asked whether damage to HSC niches by the stem and progenitor cell depletion procedure might contribute to the loss of HSCs. Osteoblasts,^{24,25} CXCL12-abundant reticular cells,²⁶ and mesenchymal stromal cells²⁷ (supplemental Figure 1C) showed no sign of Cre-mediated recombination in *HSC-CreERT⁺R26^{EYFP/EYFP}* mice and their numbers were not altered in HSPC-depleted mice compared with controls (Figure 3A-B). Fifty percent of endothelial cells²⁸ (ECs) showed activation of the Cre-excision reporter and ECs were reduced by 50% in HSPC-depleted animals. In order to test

whether the reduction of ECs contributed to HSPC depletion, we transplanted uninduced *HSC-CreERT⁺R26^{DTA/DTA}* mice with wt WBMcs and TAM treatment of the chimeras 10 weeks later reproduced the partial loss of ECs but showed no reduction of LT-HSCs (Figure 3C). Because TAM-induced *HSC-CreERT⁺R26^{DTA/DTA}* animals displayed massively reduced HSPC numbers, we hypothesized that these mice might be receptive for BM transplants without additional preconditioning and transferred WBMcs from congenic B6.ubiRFP donors into TAM-induced *HSC-CreERT/R26^{DTA/DTA}* recipients (Figure 3D). In contrast to *Cre⁻* control recipients, PB and BM analysis revealed a robust donor chimerism in HSPC-depleted recipients, confirming unperturbed HSC niches after HSPC depletion.

Collectively, we showed highly efficient depletion of LT-HSCs in TAM-induced *HSC-CreERT⁺R26^{DTA/DTA}* mice whereas ST-HSCs and progenitors were only moderately reduced. Important cellular constituents of the HSC niche were not affected and the temporary loss (see Figure 2A) of 50% of BM ECs was irrelevant for HSC maintenance.

After induced depletion, LT-HSCs initially reexpand but then stagnate at low numbers

To assess the duration of LT-HSC reduction, HSPC-depleted mice were sacrificed at different time points after TAM induction for BM analysis (Figure 2A). The LT-HSC population recovered initially and expanded from almost undetectable to 8% of control numbers within 6 weeks after depletion. Unexpectedly, LT-HSC numbers stagnated at this level for at least 28 weeks, whereas ECs had already recovered within 6 weeks. To test whether this persistent reduction of immunophenotypic LT-HSCs was also reflected in a loss of functional LT-HSC activity, we competitively transplanted WBMcs 17 weeks after HSPC depletion (Figure 2B; supplemental Figure 3A) and found repopulating activity severely reduced. In order to obtain an estimate of the functional HSC frequency directly after depletion as well as in the plateau phase, we transplanted limiting doses²⁹ of *HSC-CreERT⁺R26^{DTA/DTA}* WBMcs together with wt competitor cells (Figure 2C; supplemental Table 1). The HSC frequency of *Cre⁺* mice was reduced to 1% of *Cre⁻* littermate controls (*Cre⁺*, $1/6.2 \times 10^6$ WBMcs; *Cre⁻*, $1/7.0 \times 10^4$ WBMcs) directly after TAM induction, whereas the HSC frequency of mice 13 weeks after depletion had increased to 7% of controls (*Cre⁺*, $1/6.5 \times 10^5$ WBMcs; *Cre⁻*, $1/4.3 \times 10^4$ WBMcs). In a similar approach, we transplanted limiting doses of WBMcs from animals that were depleted 14 weeks earlier without additional competitor cells and estimated the HSC frequency to be $1/1.2 \times 10^6$ WBMcs (supplemental Figure 3B).

In order to rule out that the incomplete recovery of LT-HSCs was due to damage to cells providing niche space for HSCs, we performed control experiments in which we transplanted *HSC-CreERT⁺R26^{DTA/DTA}* BM cells from untreated animals into irradiated wt recipients and induced HSPC depletion only later in the chimera (Figure 2D; supplemental

Figure 2. Limited LT-HSC expansion after induced HSPC depletion. (A) *HSC-CreERT/R26^{DTA/DTA}* mice were TAM-induced (3×0.3 mg/g BW within 10 days) and analyzed for BM LT-HSC and EC counts at the indicated time points. Mean absolute LT-HSC/EC number per 2 femora of *Cre⁻* mice was set to 1 (means \pm SD, $n = 3$ -6 per group). (B) WBMcs from *HSC-CreERT/R26^{DTA/DTA}* mice isolated 17 weeks after TAM induction (see also supplemental Figure 3A) were transplanted along with B6.CD45.1-competitor WBMcs into irradiated B6.CD45.1/CD45.2 recipients. WBMcs of 3 donors per genotype were each transplanted into 2 recipients. *Cre⁺* or *Cre⁻* donor contribution to recipient PB neutrophils (NEUT, CD11b⁺Gr-1^{hi}) and lymphoid cells (LYMPH, FSC^{lo}SSC^{lo}CD11b⁺Gr-1⁺) were analyzed (means \pm SD, experiment representative of 2 individual replicates). (C) Different doses (supplemental Table 1) of *HSC-CreERT/R26^{DTA/DTA}* (*Cre⁺* or *Cre⁻*) WBMcs were transplanted either directly (left data plot) or 13 weeks (right data plot) after TAM induction alongside with B6.CD45.1-competitor WBMcs into irradiated B6.CD45.1/CD45.2 recipients. Sixteen to 22 weeks after transplantation, recipients showing $<0.01\%$ multilineage *R26^{DTA/DTA}* donor repopulation in PB were scored as negative. Frequencies of LT-HSCs and statistics (bottom) were calculated using ELDA software. (D) Irradiated congenic B6.CD45.1/CD45.2 recipients were transplanted with 6×10^4 sorted CD117⁺*lin⁻* BM donor cells from uninduced *HSC-CreERT/R26^{DTA/DTA}* (*Cre⁺* and *Cre⁻*) mice. Ten weeks after transplantation, chimeras were TAM-induced (left) and LT-HSC (LSK CD48⁻CD150⁺) numbers in 2 femora were analyzed 2 or 11 weeks after TAM induction (right). Mean absolute LT-HSC number of *Cre⁻* was set to 1 (means \pm SD, $n = 2$ -4 per group). CI, confidence interval; ln, natural logarithm.

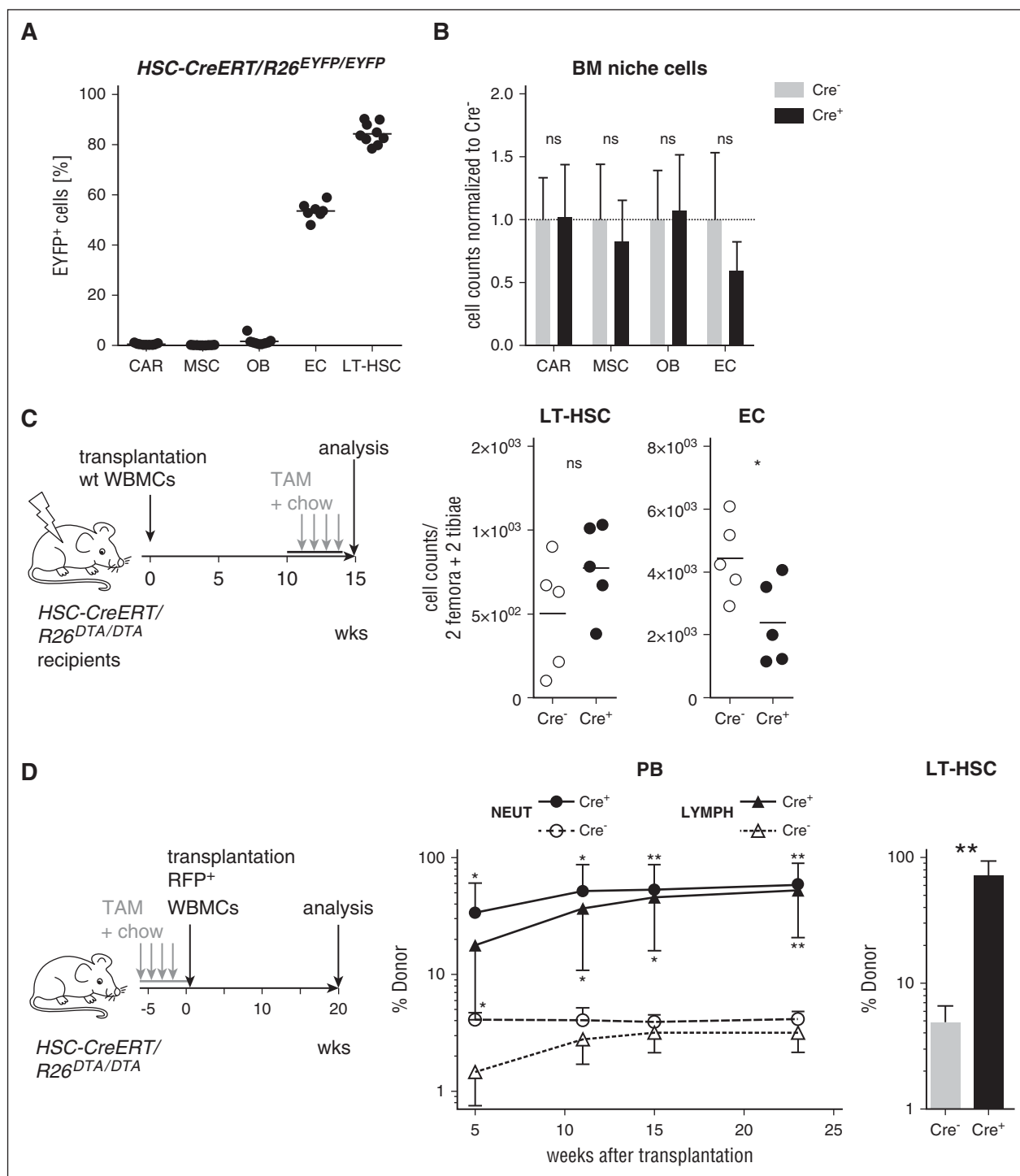


Figure 3. Effects of HSPC depletion on hematopoietic niche cells. (A) *HSC-CreERT⁺ R26^{EYFP/EYFP}* animals ($n = 7-9$ per cell population, black bars indicate means) were TAM-treated (4×0.2 mg/g BW plus TAM chow) for 4 weeks and BM niche cell subsets were analyzed for EYFP expression. BM LT-HSCs from the same animals served as a positive control for TAM induction. Identification of CXCL12-abundant reticular (CAR) cells, mesenchymal stem/progenitor cells (MSC), osteoblasts (OB), and ECs is shown in supplemental Figure 1C. (B) *HSC-CreERT/R26^{DTA/DTA}* animals ($n = 7-12$ per group) were TAM-treated (as described in panel A) and selected BM niche cell subsets were quantified by flow cytometry. Absolute cell numbers from 2 femora and 2 tibiae were determined. Mean population size of Cre⁻ controls was set to 1. Means \pm SD are shown. (C) *HSC-CreERT⁺ R26^{DTA/DTA}* (Cre⁺) and Cre⁻ control recipients (Cre⁻) were lethally irradiated and transplanted with 5×10^6 WBMcs from B6.ubiEYFP donors which were wt except for ubiquitous EYFP expression (left). Ten weeks after transfer, chimeras were TAM-induced for 4 weeks (4×0.2 mg/g BW plus TAM chow) and absolute numbers of LT-HSCs and ECs per 2 femora and 2 tibiae were determined (right); $n = 5$ per genotype, black bar mean. (D) *HSC-CreERT/R26^{DTA/DTA}* recipients ($n = 3$ to 5 per genotype) were TAM-induced for 4 weeks (4×0.2 mg/g BW and TAM chow; see also supplemental Figure 2A,C) and transplanted with 2.5×10^7 WBMcs from B6.ubiRFP donors which were wt except for ubiquitous RFP expression. PB neutrophil (NEUT, CD11b⁺ Gr-1^{hi}) and lymphoid cell (LYMPH, FSC^{lo}SSC^{lo}CD11b⁻ Gr-1⁻) chimerism (middle) were monitored thereafter and BM donor chimerism (right) was analyzed 23 weeks after transfer. Experiment is representative of 2 individual replicates.

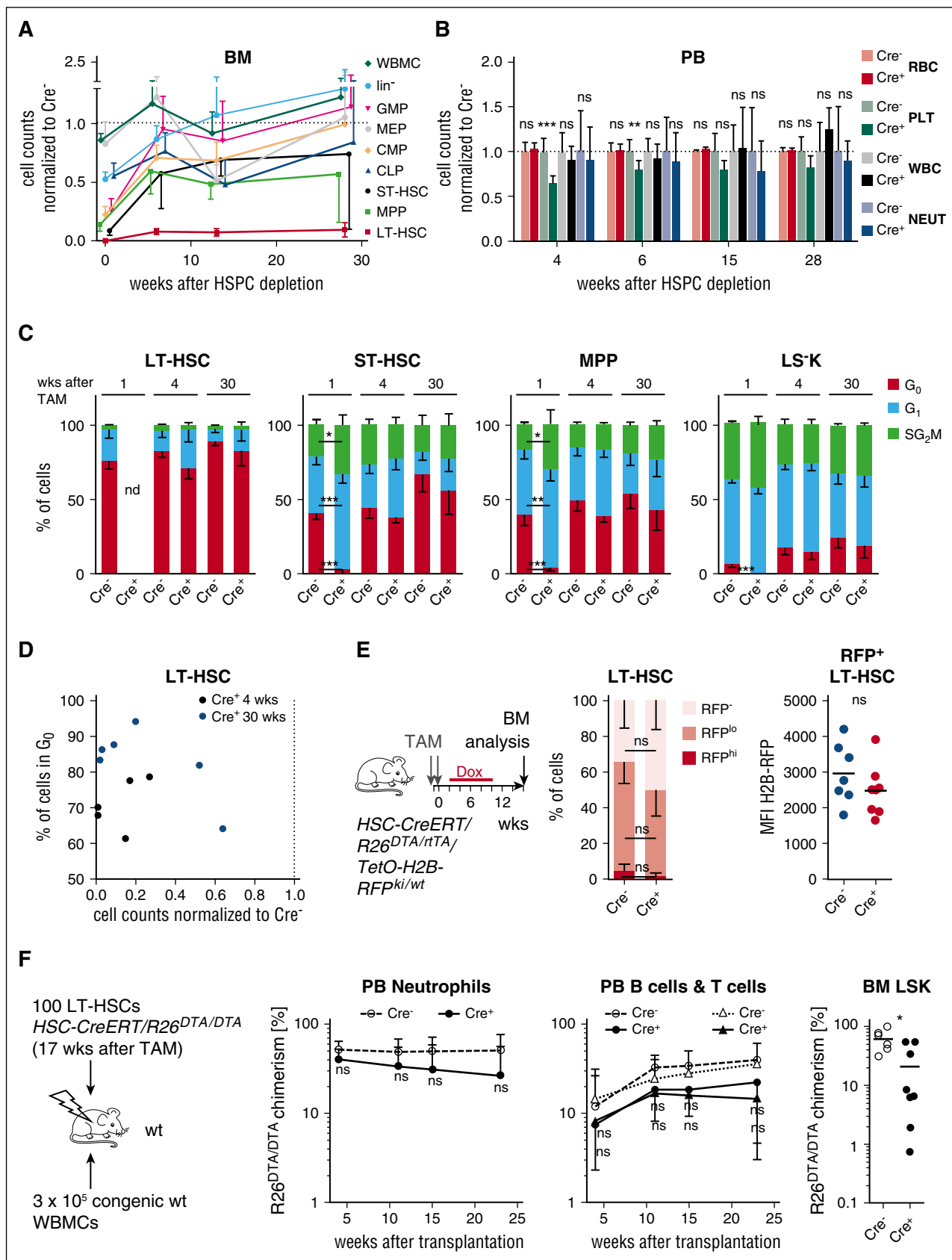


Figure 4. Persistently low LT-HSC numbers do not impair steady-state hematopoiesis. (A) HSC and precursor populations in the BM of TAM-treated *HSC-CreERT/R26^{DTA/DTA}* mice were analyzed at the indicated time points (as in Figure 2A). Absolute size of populations per 2 femora of Cre⁺ animals (n = 4-6 per time point) were normalized to the respective mean of Cre⁻ controls (n = 3-5 per time point, not shown), which was set to 1 (dotted line). Means ± SD of Cre⁺ are shown. (B) Numbers (count per microliter) of WBC and red blood cells (RBC), platelets (PLT), and neutrophils (NEUT) in PB of HSPC-depleted *HSC-CreERT/R26^{DTA/DTA}* and Cre⁻ controls were

Figure 3C). Also, this setup did not result in HSC recovery. The limited LT-HSC recovery in HSPC-depleted mice was not caused by persistent bioactivity of TAM³⁰ as determined by transplantation of uninduced *HSC-CreERT⁺/R26^{YFP/wt}* WBCs into previously TAM-treated wt recipients (supplemental Figure 3D).

Collectively, upon induced depletion in adult mice, LT-HSCs initially reexpanded for some weeks, but then stagnated at <10% of normal numbers as shown immunophenotypically and functionally.

Persistently low LT-HSC numbers do not impair hematopoiesis

To address effects of the prolonged LT-HSC reduction on hematopoiesis, we assessed numbers of precursor and mature blood cells of the HSPC-depleted animals shown in Figure 2A. After induced HSPC depletion, progenitor populations also showed variable reduction, but in contrast to LT-HSCs rapidly recovered. While erythromyeloid progenitors, *lin*[−] and WBCs reached the range of controls within 6 to 13 weeks after TAM induction (Figure 4A; supplemental Figure 4D), ST-HSCs and MPPs had recovered to 50% of normal numbers by this time. Consistent with substantial recovery of BM precursors, numbers of mature cells in PB (Figure 4B; supplemental Figure 4A) and spleen (supplemental Figure 4B) did not evidence hematopoietic failure for at least 50 weeks after TAM induction. We found no signs of compensatory extramedullary hematopoiesis in HSPC-depleted mice (supplemental Figure 4C).

We next asked whether the few residual HSCs compensated for the loss of the bulk of the population by rapid proliferation and determined cell-cycle activity 1, 4, and 30 weeks after TAM induction (Figure 4C; supplemental Figure 4D). One week after HSPC depletion, all hematopoietic progenitor cells were rapidly cycling, whereas analysis of residual LT-HSCs was precluded by their low abundance. At later time points, the majority of residual LT-HSCs remained quiescent and the distribution of cells in G₀, G₁, and S/G₂/M phase did not significantly differ from Cre[−] littermate controls. Moreover, cell-cycle activity of residual LT-HSCs did not correlate with the severity of LT-HSC depletion (Figure 4D). In order to quantify cumulative proliferation of residual LT-HSCs after depletion, we generated *HSC-CreERT/R26^{DTA/rTA}/Col1A1^{1tetO-H2B-RFP/wt}* mice. In these animals, expression of a fluorescent histone H2B-RFP fusion protein can be induced Cre-independently by Dox administration. After withdrawal of Dox, retention of this label identifies quiescent cells.^{4,5,31} We TAM-induced *HSC-CreERT/R26^{DTA/rTA}/Col1A1^{1tetO-H2B-RFP/wt}* animals, subsequently pulsed them with Dox (Figure 4E), and analyzed the BM after 6 weeks of chase. Frequencies of LT-HSCs retaining or diluting the label (Figure 4E; supplemental Figure 4E) were not significantly different between HSPC-depleted animals and Cre[−] littermates. Based on median fluorescence intensity and frequency of RFP⁺ LT-HSCs, we estimated that residual LT-HSCs from depleted animals underwent on average less than a single (~0.5-0.8; see supplemental Figure 4F) additional cell division within 6 weeks of chase compared with LT-HSCs from control mice.

In order to address the functionality of residual LT-HSCs, we transplanted LSK CD48[−]CD150⁺CD34[−]CD135[−] cells isolated from *HSC-CreERT/R26^{DTA/DTA}* mice that were TAM-induced 17 weeks before along with competitor wt WBCs (Figure 4F). Donor contribution to PB of chimeric recipients was inhomogeneous among donor LT-HSCs isolated from individual Cre⁺ mice and BM analysis after 23 weeks revealed a significant reduction of repopulation activity. The repopulation potential did not correlate with the size of the residual LT-HSC population (supplemental Figure 4G).

In summary, we found quick and substantial recovery of hematopoietic progenitor populations and normal numbers of mature blood cells in HSPC-depleted mice. The repopulation activity of the residual HSC pool was inhomogeneous and reduced, albeit present. In contrast to this, we found no evidence for strongly increased proliferation of residual LT-HSCs as a compensatory mechanism.

Hematopoietic stress is well tolerated in spite of low HSC numbers

In order to test whether HSPC-depleted mice can acutely increase their mature blood cell output, we applied different hematopoietic stressors. Hemolytic anemia was induced by PHZ injection (Figure 5A; supplemental Figure 5A). In HSPC-depleted mice, hematocrit and erythrocyte numbers as well as physical constitution showed a similar recovery compared with control mice and both groups featured comparable increases in PB reticulocytes and BM erythroid progenitors.³² Likewise, thrombocyte numbers rapidly recovered with similar kinetics in both groups after induced depletion by injection of antiplatelet serum (Figure 5B). BM analysis 6 days after treatment revealed persistently low HSC numbers in Cre⁺ animals, whereas progenitors were not significantly altered.

Next, we challenged HSPC-depleted and control mice by administration of G-CSF, which causes cell-cycle entry, as well as mobilization and myeloid differentiation of HSCs and progenitor cells.³³ G-CSF was administered for 5 consecutive days (Figure 5C) and accelerated blood cell generation (supplemental Figure 5B) and mobilized LT-HSCs to the periphery in both groups (Figure 5C). BM analysis of HSPC-depleted mice 2 weeks after treatment revealed that G-CSF treatment had not stimulated expansion of HSC numbers as judged by immunophenotype and repopulation activity (Figure 5C; supplemental Figure 5C). We also treated HSPC-depleted mice and controls with the type I interferon inducer pI:C, which causes HSC activation.⁶ pI:C treatment was well tolerated and did not result in LT-HSC expansion in HSPC-depleted mice (supplemental Figure 5D).

We next challenged HSPC-depleted and control mice with a single dose of 5-FU, which eliminates cycling cells. Six days after 5-FU, mice of both groups showed severe loss of platelets (PLTs), reticulocytes, and white blood cells (WBCs), as expected (Figure 5D; supplemental Figure 5E). At day 13, both groups had recovered as judged by PB and

Figure 4 (continued) determined at different time points after TAM treatment (as in Figure 2A). Cre[−] control means were set to 1 (means ± SD, n = 3-13 per group). (C) Frequencies (means ± SD are shown) of LT-HSCs, ST-HSCs, MPPs, and LSK cells in G₀, G₁, and S/G₂/M phase were determined by Ki67 expression and DNA content analysis (see supplemental Figure 1D) 1, 4, and 30 weeks after TAM. Cell-cycle analysis of LT-HSCs isolated from Cre⁺ mice 1 week after depletion was not possible due to very low abundance of these cells. Only significant results are indicated. (D) Correlation of LT-HSCs in G₀ (%) and HSC-depletion efficiency (cell counts normalized to Cre[−] controls, mean set to 1) from Cre⁺ individuals 4 (black) and 30 (blue) weeks after TAM induction. (E) *HSC-CreERT/R26^{DTA/rTA}/Col1A1^{1tetO-H2B-RFP/wt}* mice were TAM-treated (2 × 0.2 mg/g BW) and H2B-RFP expression was induced by Dox treatment. Cre⁺ (n = 8) and Cre[−] animals (n = 7) were chased for 6 weeks and H2B-RFP label retention in BM LT-HSCs was analyzed. Frequencies (mean ± SD) of LT-HSCs retaining high (RFP^{hi}) or low (RFP^{lo}) level or complete dilution (RFP[−]) of H2B-RFP are shown. Median H2B-RFP fluorescence intensities (MFI) of RFP⁺ LT-HSCs from individual mice are shown (see supplemental Figure 4E for RFP gating of LT-HSCs). (F) One hundred LSK CD48[−]CD150⁺CD34[−]CD135[−] cells were sorted from individual HSPC-depleted mice (Cre⁺, n = 8) or controls (Cre[−], n = 6) 17 weeks after TAM induction and transplanted together with 3 × 10⁵ B6.CD45.1 competitor WBCs into lethally irradiated recipients (a single recipient mouse for each donor). Neutrophil, B-cell, and T-cell donor chimerism was measured in PB. Donor chimerism of LSK cells in recipient BM was analyzed 23 weeks after transfer. Means ± SD are shown.

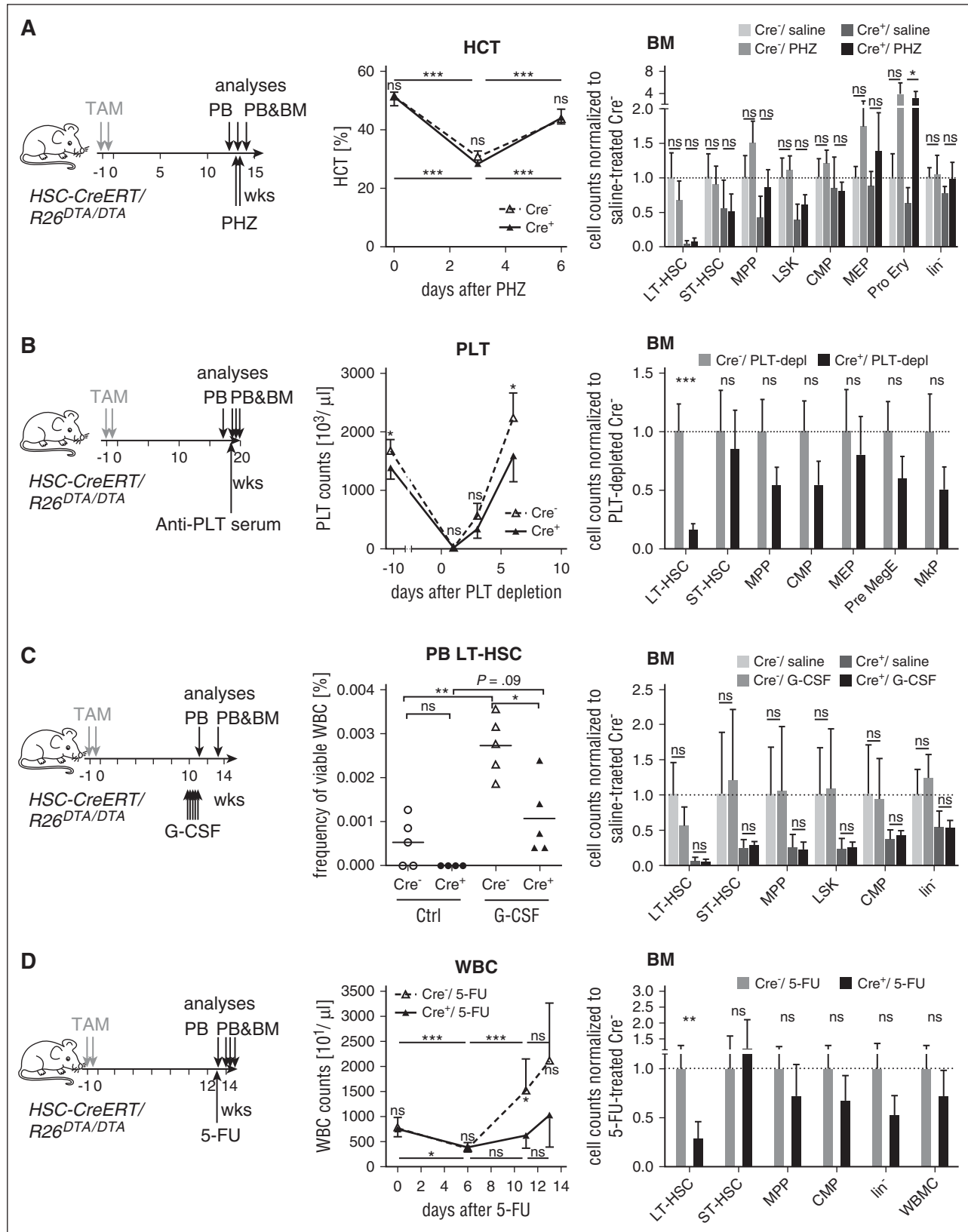


Figure 5. Low HSC numbers are sufficient to meet acutely increased demand for mature blood cells. (A) *HSC-CreERT/R26^{DTA/DTA}* mice ($n = 4-7$ per group) were TAM-treated (2×0.2 mg/g BW) and 12 weeks later injected with PHZ or saline. PB hematocrit (HCT) was measured directly before PHZ injection and 3 and 6 days afterward (middle). One week after PHZ injection, BM populations from 2 femora were quantified by flow cytometry (right). Mean \pm SD, absolute counts from 2 femora were normalized to the mean of saline-treated Cre⁻ controls (dotted line). (B) *HSC-CreERT/R26^{DTA/DTA}* animals were TAM-treated (2×0.1 mg/g BW) and 19 weeks later i.p. injected with antiplatelet serum. Platelet (PLT) counts in PB were measured at the indicated time points before and after platelet depletion. HSC and progenitor populations in the BM were analyzed 6 days after PLT depletion (PLT-depl). Mean \pm SD, absolute counts from 2 femora, normalized to the mean of Cre⁻ controls (dotted line). (C) *HSC-CreERT/R26^{DTA/DTA}*

macroscopic parameters. PB cell generation of the HSPC-depleted cohort, however, recovered with significant delay. Despite low HSCs numbers in these mice, progenitor counts were already in the range of controls at this time point. In a second experiment with more efficient depletion and earlier application of 5-FU (supplemental Figure 5F), hematopoiesis failed in HSPC-depleted animals.

In summary, hematopoietic stress was tolerated by HSPC-depleted mice and did not induce reexpansion of LT-HSC numbers. However, 5-FU–induced myeloablation was compensated with delay or was lethal in HSPC-depleted animals.

Discussion

A majority of HSCs were reported to actively contribute to hematopoiesis in steady state.^{4,5,34} However, 2 recent publications^{9,10} reported, based on HSC fate-tracking experiments, that LT-HSCs only marginally contribute to steady-state hematopoiesis. Busch et al predicted that hematopoiesis might proceed normally in the absence of LT-HSCs.¹⁰ We directly demonstrated that a 15-fold reduction of LT-HSCs did not result in detectable hematopoietic failure for at least 1 year. Moreover, this reduction did not lead to significantly increased cell-cycle activity of the few remaining LT-HSCs. We showed that the residual quiescent LT-HSCs undergo less than a single additional cell division within 6 weeks. The input from remaining LT-HSCs to downstream progenitor compartments was therefore strongly reduced in HSPC-depleted mice vs controls. In spite of this reduced total input from LT-HSCs, steady-state hematopoiesis was not compromised. Moreover, cell-cycle activity of residual LT-HSCs did not correlate with depletion efficiency, arguing against compensation of LT-HSC depletion by increased proliferation of the few remaining HSCs.

Depending on the intensity of the depletion protocol, LT-HSCs were reduced to minimal or undetectable numbers in the first days after depletion as determined by immunophenotype and competitive repopulation assays. The population showed some initial recovery within the next few weeks but then stagnated below 10% of normal numbers for up to 28 weeks. It is likely that the few residual LT-HSCs (~50 HSCs per mouse, assuming a total BM cellularity of 3×10^8 per mouse³⁵ and an initial HSC frequency of 1 in 6.2×10^6 WBCs), which had escaped induced elimination, partially replenished the LT-HSC pool initially after HSPC depletion. This partial expansion may account for the reduced repopulation activity upon transplantation of purified HSCs from depleted donor mice as proliferative history was shown to be critical for repopulation potential of HSCs.^{4,5,31} Earlier studies^{36–38} reported that upon transplantation into irradiated or kit hypomorphic recipients, LT-HSCs do expand initially but never arrive at LT-HSC numbers of normal mice. Our data clearly show that the limited LT-HSC expansion was not a peculiarity of transplantation into irradiated or kit-deficient hosts but rather reflects an inherent property of LT-HSCs in their physiological niche. This limited HSC reexpansion was not observed in an earlier report of HSPC depletion using a

CD117-blocking antibody.³⁹ In this study, immunophenotypic LT-HSCs fully recovered within 23 days after treatment, but the recovery of functional HSC activity was not analyzed. The persistent depletion of immunophenotypic and functional LT-HSCs in our study was neither caused by CreERT-mediated genotoxicity, long half-life of TAM or its metabolites, ligand-independent CreERT activation nor by damage to hematopoietic niche cells.

We hypothesize that the initial HSC expansion ceases as soon as the demand for new blood cells is met by the hematopoietic system. Even exposure of HSPC-depleted mice to hematopoietic stress and challenges reported to recruit quiescent HSCs into cycle, including 5-FU,⁴⁰ G-CSF,⁸ or pI:C,⁶ did not result in expansion of the LT-HSC compartment to its normal size. The reason for limited expansion of LT-HSCs could lie in the absence of proliferative stimuli for these cells, divisions of which must be restricted to a minimum required for efficient hematopoiesis in order to protect them against accumulation of replication-associated DNA damage and exhaustion.⁴¹

In contrast to the very limited reexpansion of HSCs, the different progenitor populations showed rapid and robust recovery after HSPC depletion. This finding argues for potent self-renewal capacity of primitive progenitors in situ, which has been underrated so far by classical transplantation experiments.

We report that ablation of mature blood cells including erythrocytes and platelets as well as enforced myeloablation by G-CSF administration was tolerated by HSPC-depleted mice. These findings question the necessity of LT-HSC activation to acutely provide an influx of progenitor cells in situations of increased demand for blood cells. Only elimination of the majority of cycling cells by 5-FU compromised the hematopoietic system of HSPC-depleted animals, demonstrating that normal numbers of HSCs and progenitors are essential to cope with myeloablation. This observation did not result from increased sensitivity of HSCs and progenitor cells to 5-FU in HSPC-depleted mice, as these cells remain quiescent despite depletion. Our experiments do not resolve whether myeloablation by 5-FU is compensated primarily by LT-HSCs or rather by progenitors or both.

If hematopoiesis proceeds normally despite reduction of LT-HSCs to below 10% of physiological numbers, why is the hematopoietic system equipped with so many of these cells? The function of the large size of the LT-HSC pool may be to maintain a low-level input of new progenitor cells from the LT-HSC compartment for the lifespan of the animal with only minimal numbers of cell divisions demanded from an individual HSC, protecting it from replication-associated DNA damage. An explanation for the continuous low-level activity and contribution of LT-HSCs would be the need for constant cell-cycle entry to maintain genomic integrity as exit from quiescence was shown to promote error-free DNA damage repair,⁴² whereas quiescence favors error-prone repair mechanisms.⁴³

For the first time, we directly show that the majority of the LT-HSC population is dispensable for steady-state hematopoiesis and that blood cell generation can be maintained by progenitor cells with minimal input from residual HSCs. Our finding that acute hematopoietic stressors were tolerated by HSPC-depleted mice further proves the so far underrated regenerative capacity of progenitor cells.

Figure 5 (continued) mice ($n = 4-5$ per group) were TAM-induced and 10 weeks later injected with G-CSF or saline. PB was analyzed 1 day after the last injection for immunophenotypic LT-HSCs (middle). Two weeks after G-CSF treatment BM populations from 2 femora were quantified by flow cytometry (right, normalization and display as in panel A). (D) *HSC-CreERT⁺R26^{DTA/DTA}* (Cre^{+} , $n = 3-5$) and control mice (Cre^{-} , $n = 4-9$) were TAM-induced (2×0.2 mg/g BW) and 13 weeks later injected IV with 5-FU or saline. PB WBC counts of 5-FU–treated mice were determined at the indicated time points (middle data plot, means \pm SD, Cre^{+} , red; Cre^{-} , dotted black line). BM populations of *HSC-CreERT⁺R26^{DTA/DTA}* and Cre^{-} control mice were measured 13 days after 5-FU injection. Means \pm SD are shown; absolute counts from 2 femora were normalized to the mean of 5-FU–treated Cre^{-} controls. For data of saline-treated controls, refer to supplemental Figure 5E. Ctrl, control; MkP, megakaryocyte progenitor; Pre MegE (see Pronk et al³² for description); Pro Ery, proerythroblast.

Acknowledgments

The authors thank Livia Schulze, Christa Haase, Tobias Häring, Doreen Ussath, and Christina Hiller for expert technical assistance; Frank Buchholz, Sebastian Gerdes, Cristina Lo Celso, and Werner Müller for scientific discussions; and Nicole Mende for help with niche cell analysis.

This work was supported by the German Research Foundation (Deutsche Forschungsgemeinschaft [DFG]) through grant SFB 655 B11 (A.R.), the Excellence Initiative of the German federal and state governments “Support the best” (ZUK64) (A.R.), and Technische Universität Dresden Medical Faculty “MeDDrive 2012 & 2015” grants (A.G.). K.B.S. was awarded a fellowship from the Dresden International PhD program. C.W. was supported by DFG WA2837, SFB-655 B9, FOR2033-A03, and by funding from European Union 7th FP, grant no. 261387 (CELL-PID). T.G. was supported by Fritz Thyssen Stiftung (10.14.2.153) and DFG (GR 4857/1-1).

T.Z. was supported by the German Federal Ministry of Research and Education, grant no. 031A315 (MessAge) and grant no. 031A424 (HaematoOpt).

Authorship

Contribution: K.B.S., A.G., and M.N.F.M. performed experiments; A.G. and K.B.S. designed experiments and analyzed data; T.Z. and I.R. performed statistical analysis; D.V. and J.R.G. provided essential materials; T.G. and J.R.G. discussed data; C.W. advised the study; and A.G. and A.R. conceived the study and wrote the manuscript.

Conflict-of-interest disclosure: The authors declare no competing financial interests.

Correspondence: Alexander Gerbaulet, Institute for Immunology, Carl Gustav Carus Faculty of Medicine, Technische Universität Dresden, Fetscherstr 74, 01307 Dresden, Germany; e-mail: alexander.gerbaulet@tu-dresden.de.

References

- Weissman IL. Stem cells: units of development, units of regeneration, and units in evolution. *Cell*. 2000;100(1):157-168.
- Eaves CJ. Hematopoietic stem cells: concepts, definitions, and the new reality. *Blood*. 2015; 125(17):2605-2613.
- Purton LE, Scadden DT. Limiting factors in murine hematopoietic stem cell assays. *Cell Stem Cell*. 2007;1(3):263-270.
- Wilson A, Laurenti E, Oser G, et al. Hematopoietic stem cells reversibly switch from dormancy to self-renewal during homeostasis and repair. *Cell*. 2008;135(6):1118-1129.
- Foudi A, Hochedlinger K, Van Buren D, et al. Analysis of histone 2B-GFP retention reveals slowly cycling hematopoietic stem cells. *Nat Biotechnol*. 2009;27(1):84-90.
- Essers MAG, Offner S, Blanco-Bose WE, et al. IFN α activates dormant hematopoietic stem cells in vivo. *Nature*. 2009;458(7240):904-908.
- Baldrige MT, King KY, Boles NC, Weksberg DC, Goodell MA. Quiescent hematopoietic stem cells are activated by IFN- γ in response to chronic infection. *Nature*. 2010;465(7299):793-797.
- Morrison SJ, Wright DE, Weissman IL. Cyclophosphamide/granulocyte colony-stimulating factor induces hematopoietic stem cells to proliferate prior to mobilization. *Proc Natl Acad Sci USA*. 1997;94(5):1908-1913.
- Sun J, Ramos A, Chapman B, et al. Clonal dynamics of native haematopoiesis. *Nature*. 2014;514(7522):322-327.
- Busch K, Klapproth K, Barile M, et al. Fundamental properties of unperturbed haematopoiesis from stem cells in vivo. *Nature*. 2015;518(7540):542-546.
- Voehringer D, Liang H-E, Locksley RM. Homeostasis and effector function of lymphopenia-induced “memory-like” T cells in constitutively T cell-depleted mice. *J Immunol*. 2008;180(7):4742-4753.
- Göthert JR, Gustin SE, Hall MA, et al. In vivo fate-tracing studies using the Scl stem cell enhancer: embryonic hematopoietic stem cells significantly contribute to adult hematopoiesis. *Blood*. 2005; 105(7):2724-2732.
- Srinivas S, Watanabe T, Lin CS, et al. Cre reporter strains produced by targeted insertion of EYFP and ECFP into the ROSA26 locus. *BMC Dev Biol*. 2001;1:4.
- Lucas H, Weber O, Nageswara Rao T, Blum C, Fehling HJ. Faithful activation of an extra-bright red fluorescent protein in “knock-in” Cre-reporter mice ideally suited for lineage tracing studies. *Eur J Immunol*. 2007;37(1):43-53.
- Morse HC III. Genetic nomenclature for loci controlling surface antigens of mouse hemopoietic cells. *J Immunol*. 1992;149(10):3129-3134.
- Egli D, Rosains J, Birkhoff G, Eggan K. Developmental reprogramming after chromosome transfer into mitotic mouse zygotes. *Nature*. 2007; 447(7145):679-685.
- Lallemant Y, Luria V, Haffner-Krausz R, Lonai P. Maternally expressed PGK-Cre transgene as a tool for early and uniform activation of the Cre site-specific recombinase. *Transgenic Res*. 1998; 7(2):105-112.
- Hu Y, Smyth GK. ELDA: extreme limiting dilution analysis for comparing depleted and enriched populations in stem cell and other assays. *J Immunol Methods*. 2009;347(1-2):70-78.
- Nakamura Y, Arai F, Iwasaki H, et al. Isolation and characterization of endosteal niche cell populations that regulate hematopoietic stem cells. *Blood*. 2010;116(9):1422-1432.
- Kiel MJ, Yilmaz ÖH, Iwashita T, Yilmaz OH, Terhorst C, Morrison SJ. SLAM family receptors distinguish hematopoietic stem and progenitor cells and reveal endothelial niches for stem cells. *Cell*. 2005;121(7):1109-1121.
- Adolfsson J, Borge OJ, Bryder D, et al. Upregulation of Flt3 expression within the bone marrow Lin(-)Sca1(+)-c-kit(+) stem cell compartment is accompanied by loss of self-renewal capacity. *Immunity*. 2001;15(4):659-669.
- Akashi K, Traver D, Miyamoto T, Weissman IL. A clonogenic common myeloid progenitor that gives rise to all myeloid lineages. *Nature*. 2000; 404(6774):193-197.
- Sánchez M, Göttgens B, Sinclair AM, et al. An SCL 3' enhancer targets developing endothelium together with embryonic and adult haematopoietic progenitors. *Development*. 1999;126(17):3891-3904.
- Calvi LM, Adams GB, Weibrecht KW, et al. Osteoblastic cells regulate the haematopoietic stem cell niche. *Nature*. 2003;425(6960):841-846.
- Zhang J, Niu C, Ye L, et al. Identification of the haematopoietic stem cell niche and control of the niche size. *Nature*. 2003;425(6960):836-841.
- Sugiyama T, Kohara H, Noda M, Nagasawa T. Maintenance of the hematopoietic stem cell pool by CXCL12-CXCR4 chemokine signaling in bone marrow stromal cell niches. *Immunity*. 2006;25(6):977-988.
- Méndez-Ferrer S, Michurina TV, Ferraro F, et al. Mesenchymal and hematopoietic stem cells form a unique bone marrow niche. *Nature*. 2010; 466(7308):829-834.
- Ding L, Saunders TL, Enikolopov G, Morrison SJ. Endothelial and perivascular cells maintain hematopoietic stem cells. *Nature*. 2012; 481(7382):457-462.
- Szilvassy SJ, Humphries RK, Lansdorf PM, Eaves AC, Eaves CJ. Quantitative assay for totipotent reconstituting hematopoietic stem cells by a competitive repopulation strategy. *Proc Natl Acad Sci USA*. 1990;87(22):8736-8740.
- Sánchez-Aguilera A, Arranz L, Martín-Pérez D, et al. Estrogen signaling selectively induces apoptosis of hematopoietic progenitors and myeloid neoplasms without harming steady-state hematopoiesis. *Cell Stem Cell*. 2014;15(6):791-804.
- Qiu J, Papatsenko D, Niu X, Schaniel C, Moore K. Divisional history and hematopoietic stem cell function during homeostasis. *Stem Cell Rep*. 2014;2(4):473-490.
- Pronk CJH, Rossi DJ, Månsson R, et al. Elucidation of the phenotypic, functional, and molecular topography of a myeloerythroid progenitor cell hierarchy. *Cell Stem Cell*. 2007; 1(4):428-442.
- Winkler IG, Pettit AR, Raggatt LJ, et al. Hematopoietic stem cell mobilizing agents G-CSF, cyclophosphamide or AMD3100 have distinct mechanisms of action on bone marrow HSC niches and bone formation. *Leukemia*. 2012; 26(7):1594-1601.
- Cheshier SH, Morrison SJ, Liao X, Weissman IL. In vivo proliferation and cell cycle kinetics of long-term self-renewing hematopoietic stem cells. *Proc Natl Acad Sci USA*. 1999;96(6):3120-3125.
- Boggs DR. The total marrow mass of the mouse: a simplified method of measurement. *Am J Hematol*. 1984;16(3):277-286.
- Iscoe NN, Nawa K. Hematopoietic stem cells expand during serial transplantation in vivo

- without apparent exhaustion. *Curr Biol*. 1997; 7(10):805-808.
37. Pawliuk R, Eaves C, Humphries RK. Evidence of both ontogeny and transplant dose-regulated expansion of hematopoietic stem cells in vivo. *Blood*. 1996;88(8):2852-2858.
38. Boggs DR, Boggs SS, Saxe DF, Gress LA, Canfield DR. Hematopoietic stem cells with high proliferative potential. Assay of their concentration in marrow by the frequency and duration of cure of W/W^v mice. *J Clin Invest*. 1982;70(2):242-253.
39. Czechowicz A, Kraft D, Weissman IL, Bhattacharya D. Efficient transplantation via antibody-based clearance of hematopoietic stem cell niches. *Science*. 2007;318(5854):1296-1299.
40. Harrison DE, Lerner CP. Most primitive hematopoietic stem cells are stimulated to cycle rapidly after treatment with 5-fluorouracil. *Blood*. 1991;78(5):1237-1240.
41. Walter D, Lier A, Geiselhart A, et al. Exit from dormancy provokes DNA-damage-induced attrition in haematopoietic stem cells. *Nature*. 2015;520(7548):549-552.
42. Beerman I, Seita J, Inlay MA, Weissman IL, Rossi DJ. Quiescent hematopoietic stem cells accumulate DNA damage during aging that is repaired upon entry into cell cycle. *Cell Stem Cell*. 2014;15(1):37-50.
43. Mohrin M, Bourke E, Alexander D, et al. Hematopoietic stem cell quiescence promotes error-prone DNA repair and mutagenesis. *Cell Stem Cell*. 2010;7(2):174-185.